

Emergent population dynamics from behavioral optimization in the water column

Emil Friis Frølich, Uffe Høgsbro Thygesen

November 2020

Abstract

Population dynamics in the ocean are generally modelled without taking behavior into account. This in spite of the largest daily feeding times for predators, namely at dawn and dusk, being driven by behavior. The daily pattern stems from the Diel Vertical Migration (DVM). This is usually explained by prey avoiding visual predators, and visual predators seeking to find prey. We develop a game-theoretical model of predator-prey interactions in continuous time and space, finding the Nash equilibrium at every instant. By unifying results for the general resolution of polymatrix games, and a spectral discretization scheme, we can resolve the spatially continuous game nearly instantaneously. Our approach allows a unified model for the slow time-scale of population dynamics, and the fast time-scale of the vertical migration, under seasonal changes. On the behavioral time-scale, we see the emergence of a deep scattering layer from the game dynamics. On the longer time-scale of population dynamics, the introduction of optimal behavior has a strong stabilizing, compared to the model without optimal behavior. In a changing seasonal environment, we observe a change in daily migration patterns throughout the seasons, driven by changes in both population and light levels. The framework we propose can easily be adapted to population games in inhomogenous terrestrial environments, and more complex food-webs.

1 Introduction

The diel vertical migration, (DVM), is the largest migration of organisms on earth, [], dwarfing the great migrations on the african savannah and annual bird migrations, []. During the day of billions of small fish and zoo-plankton migrate from the upper layers of the ocean to the deeper, darker layers.

At dusk, the small fish and zoo-plankton begin migrating upwards again, staying in the mixed layer at night to feed. At day, the migration has been measured world-wide as the deep scattering layer, []. The migration acts as a driver of ocean population dynamics, with a majority of predator-prey interactions taking place at dusk and dawn in the mixed layer, [].

Though understanding the DVM is of central importance in understanding ocean dynamics and carbon flux, [1], the cause of the migration is not entirely clear. Performing the migration must confer some advantage, measured in terms of increased fitness. A dominating theory is that the DVM is driven by the attempt to avoid risk from visual predation, and as such is driven by the abundance of light, [2], levels (e.g., Murray et al. (1912) and Nilsson et al. (2003)).

Empirical studies show that predators generally follow their prey in their vertical migrations, Josse et al. (1998) observed the vertical movements of tuna and the sound scattering layer, and Sims et al. (2005) observed basking sharks.

The distribution of predators depends on the distribution of prey, and vice versa. In a sense, the predators and prey are playing a game of hide and seek across the water column. Viewing the DVM as an emergent phenomenon from behavioral optimization was pioneered by [3]. Qualitative characteristics of the DVM emerged purely from behavior, such as the emergence of the deep scattering layer, [4], and a mixing of predators and prey in the mixed layer at night, [5]. This was accomplished by discretizing the water column in two zones, an upper layer and a lower dark layer, and simplifying the day-night cycle into a day and night stage, neglecting dawn and dusk. With these simplifications

Advances in computational power and new modelling approaches have led to an exploration of models with continuous space and discontinuous time, [6], and fully continuous models [7]. Expanding the complexity of the models allows prediction of fine-grained dynamics of the vertical migration, such as the exact location and size of the deep scattering layer [8, 9], and the magnitude of feeding at dawn and dusk, [10] incorporate the continuous nature of the column. Generally, organisms in game-theoretical are modeled as perfectly rational actors, acting on perfect state information. This seems patently unreasonable, as fish and zooplankton do not have perfect information on the state of the water column. In addition the minor gain in fitness from the almost-perfect choice to the perfect choice seems like it would be outweighed by the higher cognitive or sensorial cost of finding the perfect strategy.

Models of optimal behavior generally do not incorporate population dynamics, with notable exceptions, [KC09]. In particular, in previous models with a continuous spatial dimension, modeling population dynamics has been infeasible, [11].

In this paper we present a new modelling approach for population games in continuous space, applied to the diel vertical migration. We rephrase the vertical game as a linear complementarity problem, [MZ91], which can be solved efficiently. The model we use for the diel is a logical continuation of the work in [12]. Our approach provides a unified framework for examining the population and behavioral time-scales. Unifying the two time-scales allows us to examine how the vertical distribution of predators and prey change throughout the seasons and how this influences the population dynamics. We investigate the length and magnitude of the feeding rates of predators and consumers at dusk and dawn in spring, summer and autumn.

Animals are not perfectly rational, as being perfectly rational is neither energetically nor physically feasible. We incorporate this feature in our model

by letting the animals maximize an expectation value with respect to their strategy, and letting their strategy incorporate noise. This allows us to examine how the optimal behavior with noise differs from that without noise, and how it changes the population dynamics. Again, this is only feasible due to the numerical scheme we have chosen to examine the system. We examine how vertical the migration patterns differ between fully rational actors, and actors with bounded rationality. A change away from full rationality is expected to impact the fitness negatively but by how much? We examine this by looking at the population dynamics for the fully rational organisms compared to those with bounded rationality. As a baseline, we compare against the system with no behavioral optimization to see how the population dynamics evolve there.

2 Model

Model introduction

We consider a food-chain in a water column, consisting of a resource R with concentration $r(z, t)$, a consumer C with concentration $c(z, t)$ and a predator with concentration $p(z, t)$. The resource is thought of as phytoplankton, the consumer as copepods and the predator as forage fish. The concentrations and total amounts are related as:

$$R(t) = \int_0^{z_0} r(z, t) dz \quad (1)$$

$$C(t) = \int_0^{z_0} c(z, t) dz \quad (2)$$

$$P(t) = \int_0^{z_0} p(z, t) dz \quad (3)$$

Forage fish are visual predators, so their predation success is heavily light dependent. The available light decreases with depth in the water column, and varies with the time of day. The light intensity I at depth z is approximately $I(z) = I_0 \exp(-kz)$, and the basic clearance rate of a predator at maximum light is $\beta_{p,0}$. However, even when there is no light available there is still a chance of catching a consumer if it is directly encountered, so the clearance rate, $\beta_p(z, t)$, of forage fish never goes to 0 even at the middle of the night or at the deepest depths.

$$\beta_p(z, t) = \beta_{p,0} \frac{I(z, t)}{1 + I(z, t)} + \beta_{p,min} \quad (4)$$

We model the light-levels at the surface via. the python package `pvlb`, using a simple Clear Sky model in Oresund between Denmark and Sweden. The light levels are given by the direct horizontal light intensity at the sea-surface, neglecting more complicated optic effects. The model takes the precipitable water w_a , and aerosol optical depth, aod . We model light decay throughout the water column as $\exp(-kz)$.

In contrast to forage fish, copepods are olfactory predators, \llbracket , and their clearance rate, β_c , is essentially independent of depth and light levels, \llbracket .

$$\beta_c(z, t) = \beta_{c,0} \quad (5)$$

The interactions between the consumer and resource are local, as are the interactions between a predator and a consumer. The local encounter rate between consumers and resources is given by $\beta_c(z, t)c(z, t)r(z, t)$, and the local encounter rate between predators and consumers is $\beta_p(z, t)c(z, t)p(z, t)$.

Population dynamics

The resource cannot move actively, so its time dynamics are naturally specified locally. The growth of the resource is modeled with a logistic growth, with a loss from grazing by consumers and diffusion from the natural movement of the water. To simplify the model, we assume interactions can be described with a Type I functional response. In natural environments, undersaturation of nutrients is the norm, \llbracket .

The total population growth of the consumer population is found by integrating the local grazing rate over the entire water column multiplied by a conversion efficiency ε , subtracting the loss from predation. The growth of the predators is given by the predation rate integrated over the water column:

$$\dot{r} = r(z, t) \left(1 - \frac{r(z, t)}{r_{max}(z)} \right) - \beta_c(z, t)c(z, t)r(z, t) + k\partial_x^2 r(z, t) \quad (6)$$

$$\dot{C} = \int_0^{z_0} \varepsilon \beta_c(z, t)c(z, t)r(z, t)dz - \int_0^{z_0} \beta_p(z, t)c(z, t)p(z, t)dz - C(t)\mu_C \quad (7)$$

$$\dot{P} = \int_0^{z_0} \varepsilon \beta_p(z, t)c(z, t)p(z, t)dz - P(t)\mu_P \quad (8)$$

The concentration of prey and predators is naturally given by a product of probability densities φ_i , $i \in \{c, p\}$, describing their location and the total amount of predators and prey.

$$c(z, t) = C(t)\varphi_c(z, t) \quad (9)$$

$$p(z, t) = P(t)\varphi_p(z, t) \quad (10)$$

Incorporating Equation (9) in Equation (6), we arrive at equations for the population dynamics governed by probability densities:

$$\dot{r} = r(z, t) \left(1 - \frac{r(z, t)}{r_{max}(z)} \right) - \beta_c(z, t)\varphi_c(z, t)C(t)r(z, t) + k\partial_x^2 r(z, t) \quad (11)$$

$$\dot{C} = C(t) \left(\int_0^{z_0} \varepsilon \beta_c(z, t)\varphi_c(z, t)r(z, t)dz - \int_0^{z_0} \beta_p(z, t)\varphi_c(z, t)p(z, t)dz - \mu_C \right) \quad (12)$$

$$\dot{P} = P(t) \left(\int_0^{z_0} \varepsilon \beta_p(z, t)c(z, t)\varphi_p(z, t)dz - \mu_P \right) \quad (13)$$

Fitness proxies and optimal strategies

The instantaneous fitness of an individual forage fish (F_p) or copepod (F_c) is given by its growth rate at that instant. As fitness is an individual measure, we arrive at the fitness by dividing the population growth rate Equation (11) by the total population.

$$F_c(\varphi_c, \varphi_p) = \int_0^{z_0} \varepsilon \beta_c(z, t) \varphi_c(z, t) r(z, t) dz \quad (14)$$

$$- P(t) \int_0^{z_0} \beta_p(z, t) \varphi_c(z, t) \varphi_p(z, t) dz \quad (15)$$

$$F_p(\varphi_c, \varphi_p) = C(t) \int_0^{z_0} \varepsilon \beta_p(z, t) \varphi_c(z, t) \varphi_p(z, t) dz \quad (16)$$

Optimal strategies:

At any instant, an organism seeks to find the strategy that maximizes its fitness. A strategy in our case is a probability distribution in the water column. The optimal strategy φ_c^* of a consumer depends on the strategy of the predators, and likewise for φ_p^* for the predators. Denoting the probability distributions on $[0, z_0]$ by $P(0, z_0)$, this can be expressed as:

$$\varphi_c^*(z, t)(\varphi_p) = \operatorname{argmax}_{\varphi_c \in P(0, z_0)} \int_0^{z_0} \varepsilon \beta_c(z, t) \varphi_c(z, t) r(z, t) dz \quad (17)$$

$$- P(t) \int_0^{z_0} \beta_p(z, t) \varphi_c(z, t) \varphi_p(z, t) dz \quad (18)$$

$$\varphi_p^*(z, t)(\varphi_c) = \operatorname{argmax}_{\varphi_p \in P(0, z_0)} C(t) \int_0^{z_0} \varepsilon \beta_p(z, t) \varphi_c(z, t) \varphi_p(z, t) dz \quad (19)$$

Consumers and predators maximize their fitness simultaneously, leading to a *Nash Equilibrium*, where neither can gain anything from diverging from their strategy. The Nash equilibrium of the instantaneous game is:

$$\varphi_c^{*, NE} = \operatorname{argmax}_{\varphi_c \in P(0, z_0)} \int_0^{z_0} \varepsilon \beta_c(z, t) \varphi_c(z, t) r(z, t) dz \quad (20)$$

$$- P(t) \int_0^{z_0} \beta_p(z, t) \varphi_c(z, t) \varphi_p^{*, NE}(z, t) dz \quad (21)$$

$$\varphi_p^{*, NE} = \operatorname{argmax}_{\varphi_p \in P(0, z_0)} C(t) \int_0^{z_0} \varepsilon \beta_p(z, t) \varphi_c^{*, NE}(z, t) \varphi_p(z, t) dz \quad (22)$$

Noisy strategies

Our model incorporates that fish are not necessarily perfectly rational, but have **bounded rationality** by letting the strategy depend on the parameter σ as well, with $\sigma = 0$ being completely rational and $\sigma = \infty$ completely irrational. Rather than choosing a precise location, an individual can choose where it diffuses around. As fish cannot swim out of the top of the ocean, nor through the

bottom, we end with the partial differential equation:

$$\partial_\sigma \varphi_i = \partial_z^2 \varphi_i \quad (23)$$

$$\partial_z \varphi_i |_{z=0} = 0 \quad (24)$$

$$\partial_z \varphi_i |_{z=z_0} = 0 \quad (25)$$

Letting φ denote the density of a standard normal distribution, Equation (23) has the solution:

$$\varphi_i(x_0, z, \sigma = 0) = \delta(z - x_0) \quad (26)$$

$$\varphi_i(x_0, z, \sigma) = \kappa(x_0) \frac{1}{\sqrt{2\sigma}} \left(\varphi\left(\frac{z - x_0}{\sqrt{2\sigma}}\right) + \varphi\left(\frac{x_0 - z}{\sqrt{2\sigma}}\right) \right) \quad (27)$$

where $\kappa(x_0)$ is a normalization parameter to ensure that f_Y is a probability density. The fundamental solution, or Greens function, is thus

$$f_Y = \kappa \frac{1}{\sqrt{2\sigma}} \left(\varphi\left(\frac{z}{\sqrt{2\sigma}}\right) + \varphi\left(\frac{-z}{\sqrt{2\sigma}}\right) \right) \quad (28)$$

If a consumer has an initial strategy defined by a random variable X_c with density f_{X_c} , to find the final strategy φ_c we need to solve Equation (23) with initial value f_{X_c} and rationality σ . This is found by convolution with the fundamental solution, ??:

$$\varphi_c = f_X * f_Y(\sigma) \quad (29)$$

Having introduced noise to the strategies of consumers and predators, we can find the Nash equilibrium of their optimal distributions without noise. We find the Nash pair by inserting Equation (29) in Equation (20) and optimizing over f_{X_i} , $i \in \{c, p\}$.

$$f_{X_c}^{*,NE} = \operatorname{argmax}_{f_{X_c} \in P(0, z_0)} \int_0^{z_0} \varepsilon \beta_c(z, t) (f_{X_c} * f_Y) r(z, t) dz \quad (30)$$

$$- P(t) \int_0^{z_0} \beta_p(z, t) (f_{X_c} * f_Y) (f_{X_p}^{*,NE} * f_Y) dz \quad (31)$$

$$f_{X_p}^{*,NE} = \operatorname{argmax}_{f_{X_p} \in P(0, z_0)} C(t) \int_0^{z_0} \varepsilon \beta_p(z, t) (f_{X_c}^{*,NE} * f_Y) (f_{X_p} * f_Y) dz \quad (32)$$

The realized distributions are found by convolution with f_Y , Equation (29) as

$$\varphi_c^{*,NE} = f_{X_c}^{*,NE} * f_Y \quad (33)$$

$$\varphi_p^{*,NE} = f_{X_p}^{*,NE} * f_Y \quad (34)$$

Spatial discretization

We discretize the interval $[0, z_0]$ with a Gauss-Lobatto grid, [Kop09]. Working on a Gauss-Lobatto grid, we are working on a grid naturally accomodated to Legendre polynomials, as the nodes correspond to zeros of Legendre polynomials.

This allows the use of spectral methods for integration and differentiation, which are fully implicit. Spectral methods are particularly well-suited to working with smooth functions, as the accuracy of integration and procedures on smooth functions improves faster than any polynomial as a function of the number of grid points, [Kop09]. We approximate pure strategy of being in a point z_i by a hat-function h_i , zero everywhere apart from z_i . Due to the non-constant interval size we need to find constants α_i so h_i integrates to 1.

$$\alpha_i \int_{z_i}^{z_{i+1}} \tilde{h}_i dz = 1 \quad (35)$$

$$\tilde{h}_i(z_{i-1}) = 0, \tilde{h}_i(z_{i+1}) = 0 \quad h_i(z) = \alpha_i \tilde{h}_i(z) \quad (36)$$

Working on a grid with N points, a strategy chosen by a consumer or predator then becomes a linear combination of hat-functions,

$$\varphi_i = \sum_{j < N} a_{j,i} h_j, \quad i \in \{c, p\} \quad (37)$$

$$\sum_{j < N} a_{j,i} = 1 \quad i \in \{c, p\} \quad (38)$$

. The strategy of a player is fully determined by the a_i 's, and using spectral integration we can easily determine integrals of the type $\int_0^{z_0} \varphi_c \varphi_p dz$

When considering non-optimal actors, we need to implement the convolution with f_Y , ???. This is by initially calculating a convolution matrix C , [], which incorporates the normalization constants $\kappa(x_0)$. Using C , we can calculate a convolution of a function f with f_Y , Equation (29) by taking the matrix-vector product with C . Thereby we get a new set of pure strategies, $\hat{h}_i = h_i * f_Y$. An added benefit of incorporating bounded rationality then becomes that our strategy profiles are guaranteed to be smooth, decreasing the number of points needed for exact evaluation of the integrals.

Finding the nash equilibrium

By discretizing space, we have reduced an uncountable strategy set to a more manageable finite amount, with pure strategies h_i , or \hat{h}_i . For brevity, we simply lump them together as e_i . The gain of a consumer playing strategy e_i against a predator playing strategy e_j can be determined as $F_c(e_i, e_j)$, and similiary for a predator. This allows us to write up payoff matrices E_c, E_p , with entry (i, j) determined through $F_k(e_i, e_j), k \in \{c, p\}$. Both payoff functions are bi-linear in the strategies, so our discretization has reduced the problem to a bimatrix game. A bimatrix game is a special case of a polymatrix game, where n players play against each other in pairwise games and the total payoff is given by the sum of the payoffs across the pairwise interactions.

Polymatrix games can be solved by passing to an equivalent linear complementarity problem, [MZ91]. In our case we have a bimatrix game, but the

approach is the same for games with more players, and has been implemented in the code. The first step is to introduce the total payoff matrix:

$$R_{init} = \begin{bmatrix} 0 & E_c \\ E_p & \end{bmatrix} \quad (39)$$

As all entries in R_{init} do not have the same sign, R_{init} is not copositive. We fix this by defining $R = R_{init} - \max(R_{init})$. Applying the results of [MZ91], to find the Nash equilibrium we need to solve the problem:

$$(Hz + q) = w \quad (40)$$

$$\langle z, w \rangle = 0 \quad (41)$$

$$z \geq 0, w \geq 0 \quad (42)$$

where

$$A = \begin{bmatrix} -1 & -1 & \dots & -1 \\ -1 & -1 & \dots & -1 \end{bmatrix} \quad (43)$$

$$q = (0 \quad \dots \quad 0 \quad -1 \quad -1) \quad (44)$$

$$H = \begin{bmatrix} -R & -A^T \\ A & 0 \end{bmatrix} \quad (45)$$

This was done through two different methods. The interior-point method as implemented in IPOPT, [WB06], called via. the auto-differentiation software CasADi [AGH⁺19], and Lemkes Algorithm implemented in the Numerics package in Siconos, [ABB⁺19].

Time evolution

We solve the time-evolution of the predator and prey populations using a semi-implicit euler scheme. At each step we find the Nash equilibrium based on the last state, and evolve the populations accordingly. The time-evolution of the resource is solved by the method of exponential time differencing, using a first-order difference, [HO10]. That is, we write up the exact formula for the solution of $r(z, t + \Delta t)$ based on $r(z, t)$

$$r(z, t_{i+1}) = \exp(\Delta t k \partial_x^2) r(z, t_i) \quad (46)$$

$$+ \int_{t_i}^{t_i + \Delta t} \exp(t' k \partial_x^2) r(z, t') \left(1 - \frac{r(z, t')}{r_{max}(z)} \right) \quad (47)$$

$$- \beta_c(z, t') \varphi_c(z, t') C(t') r(z, t') dt' \quad (48)$$

We recognize $\exp(\Delta t k \partial_x^2)$ as acting by convolution with the Greens function G of the heat equation, previously seen in the guise of f_Y , Equation (28), with

$G(k, \Delta t) = f_Y(k\Delta t)$. Doing a first order-approximation, defining

$$J(z, t_i + \Delta t) = r(z, t_i) \quad (49)$$

$$+ \left(r(z, t_i) \left(1 - \frac{r(z, t_i)}{r_{max}(z)} \right) \right) \quad (50)$$

$$- \beta_c(z, t_{i+1}) \varphi_c(z, t_{i+1}) C(t_{i+1}) r(z, t_i) \Delta t \quad (51)$$

We end with the approximation:

$$r(z, t_i + \Delta) \approx G(k, \Delta t) * J(z, t_i + \Delta t) \quad (52)$$

The choice of using an exponential integrator ensures smoothness of the solution is preserved numerically, and in general the method of exponential integrators is well-suited for stiff problems, [HO10].

Model parametrization

Following [?], and [And19], we parametrize our model in a metabolically scaled manner following Kleibers law, [?].

Precipitable water	w_a	$1 \text{ g} \cdot \text{m}^{-3}$
Aeorosol optical depth	aod	0.1
Light decay	k	0.05m^{-1}
Ocean depth	z_0	170m
Minimal attack rate	β_0	$5 \cdot 10^{-3} \text{m}^3 \text{year}^{-1}$
Consumer mass	m_c	0.05 g
Predator mass	m_p	20 g
Consumer clearance rate	β_c	$32 \text{ m}^3 \text{year}^{-1}$
Predator clearance rate	β_p	$2837 \text{ m}^3 \text{year}^{-1}$
Phytoplankton growth	λ	300 year^{-1}
Phytoplankton max	r_{max}	$10 \mathcal{N}(0, 3)$
Irrationality	σ	$160 \text{ m}^2 \text{year}^{-1}$
Diffusion rate	k	$500 \text{ m}^2 \text{year}^{-1}$

3 Results

The the difference in population dynamics between a system with no behavioral optimization, Figure 1(3), bounded rationality Figure 1(2) and full rationality Figure 1(1) is stark. The resources reach a stable level quickly in all three cases, but the populations of consumers and predators differ markedly. The difference in populations between the system with bounded rationality Figure 1(2) and the fully rational system appears to be negligible, Figure 1(1). The main driver seems to be the ability to retreat to a refuge, and not exactly how it happens. At all three points in time, consumers have a constant feeding level throughout the night Figure 2. The main feeding time for predators is at dawn and dusk, with a slight peak during the day as well, Figure 2. The length of predator feeding duration increases with the length of the night, Figure 2(2,3).

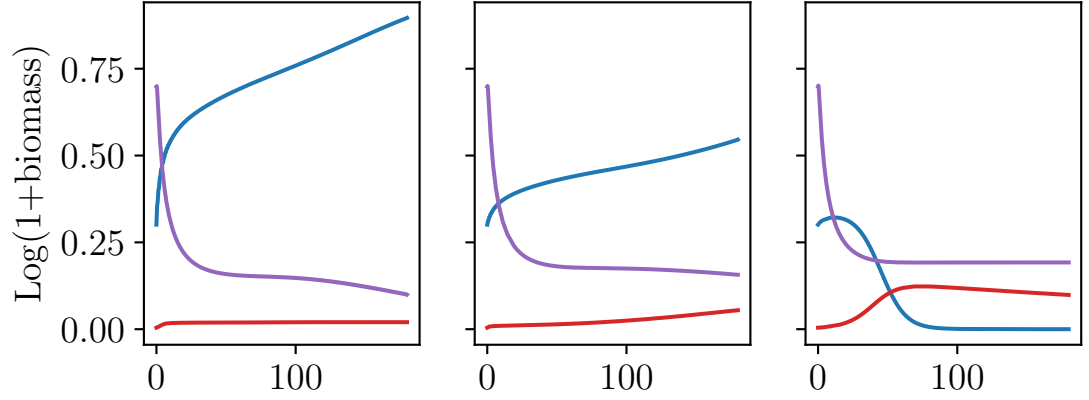


Figure 1: Total populations of consumers (*blue*), predators, (*red*) and resources (*purple*) from 1st of april to 1st of october. We vary the rationality, from total rationality (1), bounded rationality ($\sigma = 10\dots$), (2) and fully irrational, $\sigma = \infty$, (3).

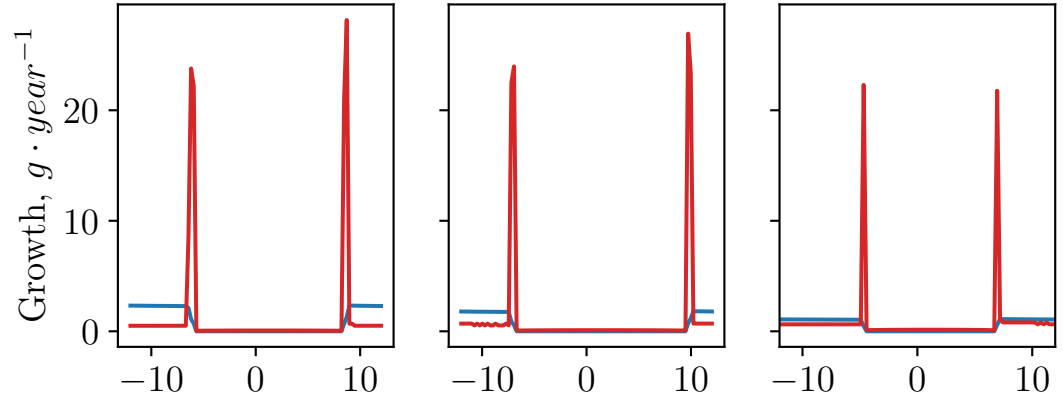


Figure 2: Seasonal comparison of consumer (*blue*) and predator, (*red*) feeding patterns on 1st of May (1), 1st of July (2) and 1st of October (3)

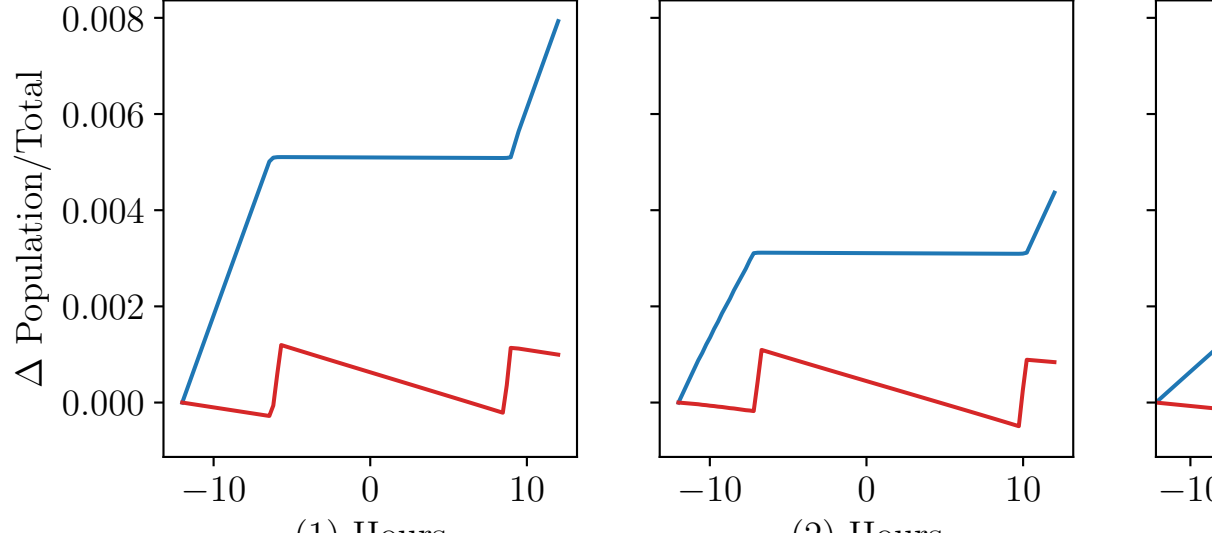


Figure 3: Comparison of consumer (*blue*) and predator, (*red*) pr. capita growth patterns with complete rationality (1), bounded rationality (2) and full irrationality (3)
To do (??)

Peak predator feeding activity decreases by a factor of 3/4 throughout the seasons, Figure 2, reflecting lower light levels. Looking at short-term population growth in the model with full rationality and bounded rationality, ?? 1(1,2), the change in consumer and predator populations throughout a day is on the order of 10^{-3} . In contrast, the model with constant behavior has rather large fluctuations of populations through a single day ?? 1(3). The driver of the daily production and growth cycles in the system with full rationality or bounded rationality is the vertical migration. Examining snapshots of the distributions, at midnight, noon, and dusk allows for a greater understanding. At midnight Figure 4(1) the consumers are concentrated near the surface, with a discontinuous drop to nothing. The predators follow the consumers, albeit with a continuous shape. At dusk, Figure 4(2) the predators have a greater concentration near the surface, while the consumer "box" is beginning to form, yet still with a continuous drop-off due to the risk from the light. At noon, Figure 4(3) the consumers form a deep scattering layer, where most of the predators are also present, excepting a few hanging out higher in the water column deterring upward consumer migration Figure 4(3)(15 m). Examining snapshots of the migration in the ecosystem with bounded rationality, Figure 5, we see roughly the same picture as in Figure 4. The greatest difference is at midnight and dusk, Figure 5(1,3), where the bounded rationality leads to a smooth shape for

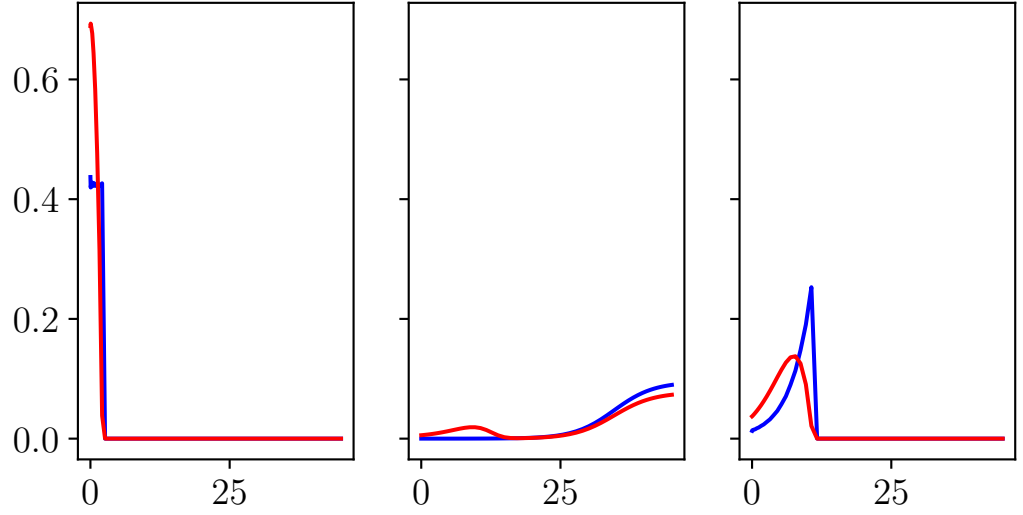


Figure 4: Daily distribution of consumers *blue* and predators *red* at midnight (1), noon (2) and at 18:45, (3) with full rationality on the 1st of October

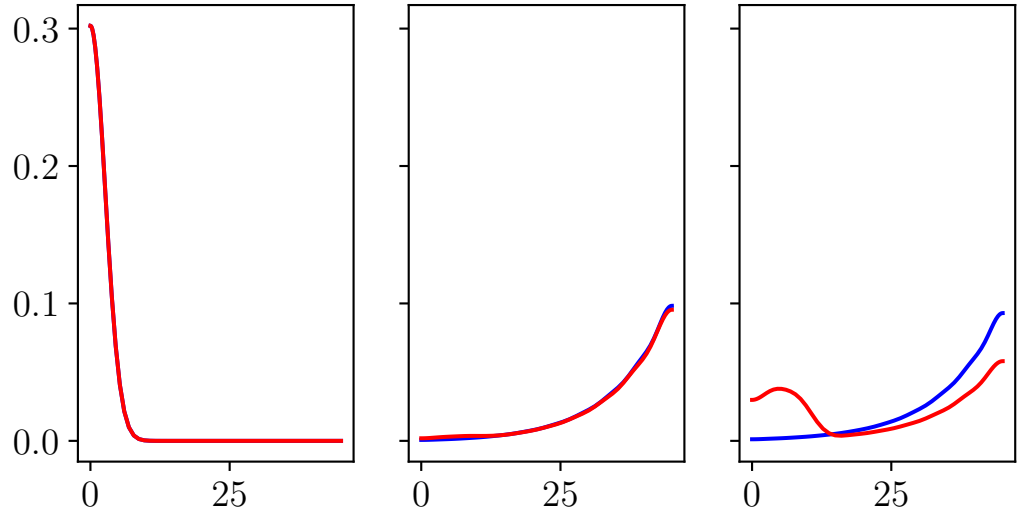


Figure 5: Daily distribution of consumers *blue* and predators *red* at midnight (1), noon (2) and at 18:45, (3) with bounded rationality

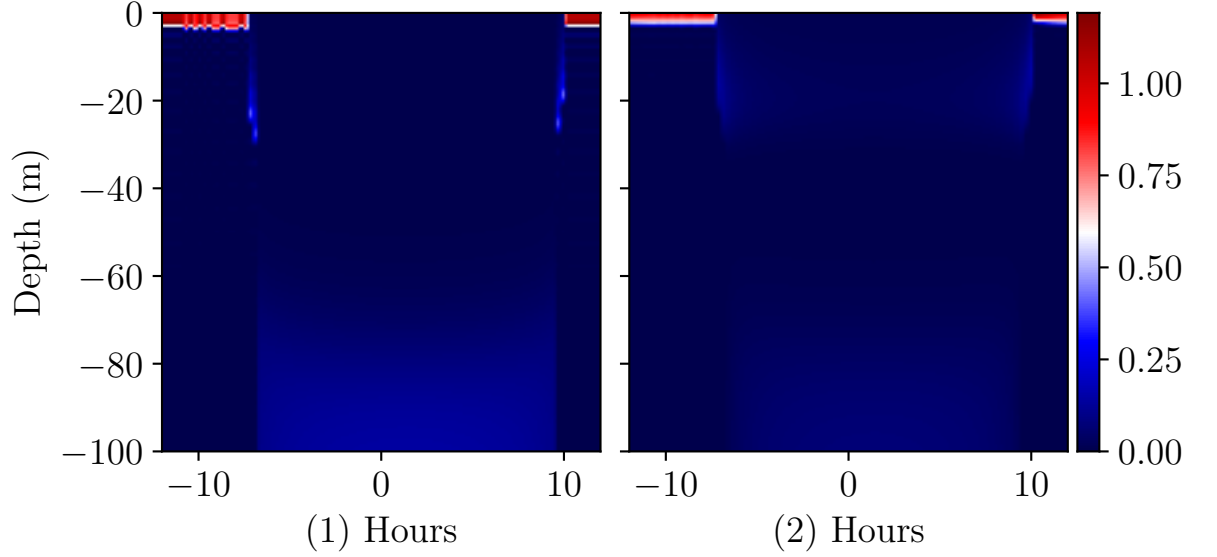


Figure 6: Vertical distribution of consumers (1) and predators (2) throughout the 1st of July. The time is in hours from noon.

the distribution of consumers. At noon, the distributions in the system with bounded rationality Figure 5(2) and Figure 4(2) are almost entirely equal. To understand the migration in greater detail, we look at the complete migration picture. The vertical migration of consumers, Figure 6(1) is clear here in the middle of the summer. They are highly concentrated at the top of the water column during nighttime, and at day they scatter throughout the deep. The pattern of the predators is slightly different from the consumer pattern, Figure 6. At nighttime there is still a non-zero concentration of predators in the upper layers of the water-column, there to catch any errant prey. Moving the hands on the clock forward to October, we again see a clearly defined vertical migration, Figure 7. The migration differs from the previous migration, in that the descent and ascent are steeper, and the distributions are wider during the night.

References

- [ABB⁺19] Vincent Acary, Olivier Bonnefon, Maurice Brémond, Olivier Huber, Franck Pérignon, and Stephen Sinclair. *An introduction to Siconos*. PhD thesis, INRIA, 2019.
- [AGH⁺19] Joel A E Andersson, Joris Gillis, Greg Horn, James B Rawlings, and Moritz Diehl. CasADi – A software framework for nonlinear opti-

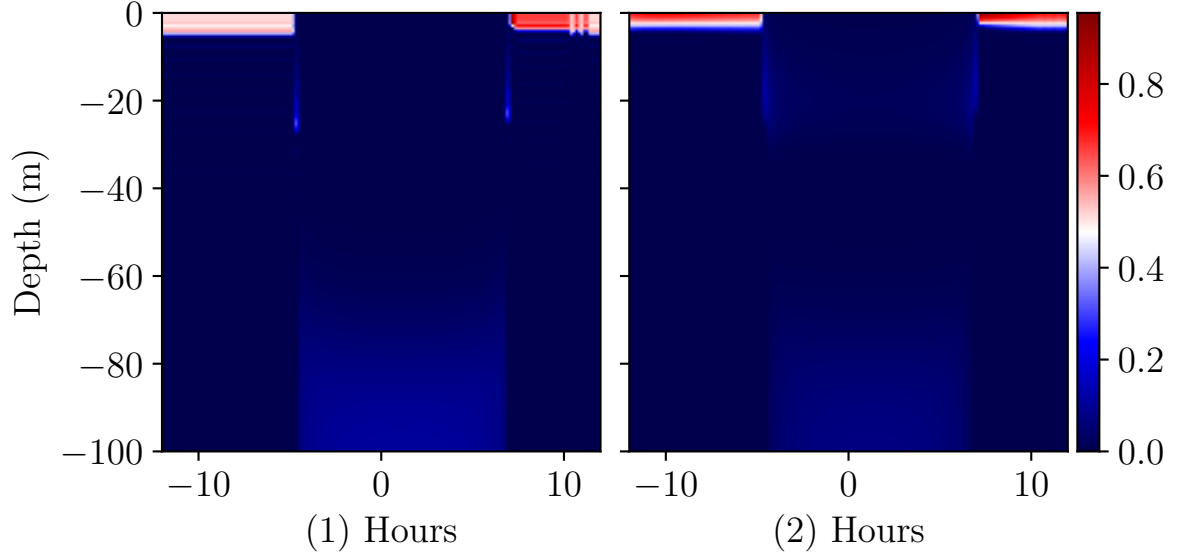


Figure 7: Vertical distribution of consumers (1) and predators (2) throughout the 1st of October. The time is in hours from noon.

mization and optimal control. *Mathematical Programming Computation*, 11(1):1–36, 2019.

- [And19] Ken H Andersen. *Fish Ecology, Evolution, and Exploitation: A New Theoretical Synthesis*. Princeton University Press, 2019.
- [HO10] Marlis Hochbruck and Alexander Ostermann. Exponential integrators. *Acta Numer.*, 19(May):209–286, 2010.
- [KC09] Vlastimil Křivan and Ross Cressman. On Evolutionary Stability in Predator-Prey Models with Fast On Evolutionary Stability in Predator-Prey Models with Fast Behavioral Dynamics Behavioral Dynamics. Technical report, 2009.
- [Kop09] David A Kopriva. *Implementing spectral methods for partial differential equations: Algorithms for scientists and engineers*. Springer Science & Business Media, 2009.
- [MZ91] Douglas A Miller and Steven W Zucker. Copositive-plus lemke algorithm solves polymatrix games. *Operations Research Letters*, 10(5):285–290, 1991.
- [WB06] Andreas Wächter and Lorenz T Biegler. On the implementation of an interior-point filter line-search algorithm for large-scale nonlinear programming. *Mathematical programming*, 106(1):25–57, 2006.